**DOI:** 10.3969/j.issn.1673-3185.2017.06.008 **http:** // english.ship-research.com

**Translated from:** XING J H, SHANG D J, ZHANG C, et al. Numerical simulation and experimental validation of characteristics of jet noise from submerged axisymmetric nozzle[J]. Chinese Journal of Ship Research, 2017, 12(6): 49-53.

# Numerical simulation and experimental validation of characteristics of jet noise from submerged axisymmetric nozzle

*XING Junhua*[1], *SHANG Dajing*[2], *ZHANG Cheng*[1], *MIAO Tiancheng*[1]

1 National Key Laboratory on Ship Vibration and Noise, China Ship Development and Design Center, Wuhan 430064, China

2 Acoustic Science and Technology Laboratory, Harbin Engineering University, Harbin 150001, China

**Abstract: [Objectives]** In order to study the underwater jet noise characteristics, **[Methods]** the Lighthill acoustic analogy is carried out to compute the underwater free jet flow sound field characteristic of axisymmetric nozzle. Applying FLUENT simulation software and large eddy simulation, the real flow field of submerged axisymmetric nozzle is simulated, and the jet noise is measured by the reverberation method. **[Results]** The results show that the core length of steady flow field is independent of the flow velocity, and the length is about 8 times the diameter of the nozzle. The radiation power of jet noise is proportional to the velocity of eight times. The differences among the radiated noise power spectra at different flow velocities are great in the low frequency, while it is significanthy reduced in the high frequency. The radiated noise energy is mainly concentrated in the low frequency. With the increase of flow velocity, the main contribution of jet noise moves to high frequency. **[Conclusions]** In terms of computing simulation of jet noise, the large eddy simulation and Lighthill acoustic analogy combined analysis is an effective means.

**Key words:** axisymmetric nozzle; jet noise; reverberation method

**CLC number:** U661.1; TB561

## 0 Introduction

Underwater radiated noise is mainly composed of mechanical noise, propeller noise, and flow noise. According to the $U^8$ law derived by Lighthill, as the fluid velocity increases, the corresponding radiated power will increase rapidly, and the flow noise will be the main source of the radiated noise[1]. At present, the research on the mechanism of underwater jet noise still stays in the theoretical level of Lighthill acoustic analogy, and there lacks perfect measurement facilities and measurement methods. Therefore, it is necessary to carry out in-depth research.

In the aspect of research on turbulence numerical simulation, Qin et al.[2] studied the effect of the size of the near-wall meshes on the turbulent calculation. Bensow et al.[3] used Large Eddy Simulation (LES) to study the viscous flow around the 2 types submarine, and verified the calculation validity of the LES by experiment.

In the aspect of research on jet noise, Stanley et al.[4] used the direct numerical simulation to study the structure and evolution process of plane jet vortexes under the low Reynolds number condition, revealed the formation and development processes of the shear layer by experiments, and obtained that, in the jet field, large-scale vortexes were anisotropic while small-scale vortexes were isotropic. Pei et al.[5] adopted the CFD technology combined with the Lighthill acoustic analogy, and found that the secondary structure of coaxial nozzle would result in the decrease in the large-scale vortexes in the shear layer and the high-frequency noise of coaxial nozzle was obviously lower than that of single nozzle. Wang et al.[6] used

**Received:** 2017-04-02

**Author(s):** XING Junhua (Corresponding author), male, born in 1982, master, senior engineer. Research interests: vibration and noise reduction of ships. E-mail: xjh0315@163.com

SHANG Dajing, male, born in 1968, associate professor. Research interest: underwater acoustic test with reverberation method. E-mail: shangdajing@hrbeu.edu.cn

the reverberation method to study the jet noise, and found that the radiation power of the jet noise decreased with the drop of the pressure head and moved towards the high frequency. Wang et al.[7] found that the vortex intensity of contraction nozzle was higher than that of annular nozzle by calculating the jet noise of different nozzles, and experimentally verified that the nozzle structure had a great effect on the radiated noise of nozzle. Through the analysis of the database of the Jet Noise Laboratory of NASA Langley Research Center, Tam et al.[8] found that the frequency structure of nozzle jet was similar. This conclusion is applicable to supersonic and subsonic jets as well as rectangular and elliptical jets.

At present, there is little research on the flow field characteristics and sound field characteristics of axisymmetric nozzle. In this paper, we will carry out numerical calculation and experimental verification on the jet noise characteristics of axisymmetric nozzle, and summarize the distributive law of the flow field and sound field of underwater jet.

# 1 Lighthill acoustic analogy

The Lighthill differential equation is the start point of the Lighthill acoustic analogy theory. The Lighthill differential equation derived from the N-S equation and the continuity equation can combine the flow field and the sound field, while the inhomogeneous term of the equation can be interpreted as the body source item. The derivation process of the Lighthill differential equation is as follows:

The continuity equation is

$$\frac{\partial \rho}{\partial t}+\frac{\partial}{\partial x_i}\left(\rho u_i\right)=0 \tag{1}$$

The N-S equation is

$$\frac{\partial}{\partial t}\left(\rho u_i\right)+\frac{\partial}{\partial x_j}\left(\rho u_i u_j\right)=-\frac{\partial P_{ij}}{\partial x_j} \tag{2}$$

where $\rho$ is the fluid density; $t$ is the time; $x_i$ and $x_j$ ($i, j$ = 1, 2, 3) are the direction coordinates in the three-dimensional Cartesian coordinate system; $u_i$ and $u_j$ are the velocity components of the fluid; $P_{ij}$ is the fluid pressure.

Taking the partial derivative of Eq. (1) with respect to time, we have

$$\frac{\partial^2 \rho}{\partial t^2}+\frac{\partial^2}{\partial t \partial x_i}\left(\rho u_i\right)=0 \tag{3}$$

Solving the divergence of Eq. (2), we have

$$\frac{\partial^2}{\partial x_i \partial t}\left(\rho u_i\right)+\frac{\partial^2}{\partial x_i \partial x_j}\left(\rho u_i u_j\right)=-\frac{\partial^2 P_{ij}}{\partial x_i \partial x_j} \tag{4}$$

Subtracting Eq. (4) from Eq. (3), we have

$$\frac{\partial^2 \rho}{\partial t^2}-\frac{\partial^2}{\partial x_i \partial x_j}\left(\rho u_i u_j\right)=\frac{\partial^2 P_{ij}}{\partial x_i \partial x_j} \tag{5}$$

Subtracting $c_0^2 \frac{\partial^2 \rho}{\partial x_i \partial x_j}$ (where $c_0$ is the sound speed of medium) from both sides of Eq. (5), we have

$$\frac{\partial^2 \rho}{\partial t^2}-c_0^2 \frac{\partial^2 \rho}{\partial x_i \partial x_j}=\frac{\partial^2}{\partial x_i \partial x_j}\left(\rho u_i u_j\right)+\frac{\partial^2 P_{ij}}{\partial x_i \partial x_j}-c_0^2 \frac{\partial^2 \rho}{\partial x_i \partial x_j}=$$
$$\frac{\partial^2}{\partial x_i \partial x_j}\left(\rho u_i u_j+P_{ij}-c_0^2 \rho\right)=\frac{\partial^2}{\partial x_i \partial x_j} \boldsymbol{T}_{ij} \tag{6}$$

where $\boldsymbol{T}_{ij}$ is the stress tensor.

All the physical quantities in the aforementioned equations are instantaneous values, i.e., the sum of fluctuating component and steady-state value. We carry out the following acoustic hypothesis for each physical quantity: The physical quantity $\rho$ in fluid mechanics can be represented by the sum of the steady-state value $\rho_0$ independent of time and the acoustic value $\rho'$ of fluctuation, i.e., $\rho=\rho_0+\rho'$.

Based on the above hypothesis, with the consideration of the fluctuating component in Eq. (6), we have that the obtained differential equation is the Lighthill equation.

$$\frac{\partial^2 \rho'}{\partial t^2}-c_0^2 \frac{\partial^2 \rho'}{\partial x_i^2}=\frac{\partial^2}{\partial x_i \partial x_j} \boldsymbol{T}_{ij} \tag{7}$$

It is supposed that the relationship between stress and strain is linear and the change in the environment parameters is neglected. Then, from Eq. (7), we can obtain the relation equation of the flow field and the sound field as follows:

$$\frac{1}{c_0^2} \frac{\partial^2 p'}{\partial t^2}-\frac{\partial^2 p'}{\partial x_i^2}=\frac{\partial^2}{\partial x_i \partial x_j} \boldsymbol{T}_{ij} \tag{8}$$

# 2 Numerical calculation

## 2.1 Flow field analysis based on CFD

In this paper, we intend to adopt the FLUENT software and LES to build a flow domain with the longitudinal section size of 360 mm × 600 mm to obtain the true time-averaged flow field, where the nozzle diameter is 10 mm. The inlet boundary condition is the speed inlet, the outlet boundary condition is the pressure outlet, and the others are non-slip wall boundary conditions. In the stage of mesh division, we densify the meshes of the nozzle and the area around it. The number of divided meshes is $8.73 \times 10^6$, the maximum skewness coefficient is 0.6, and Aspect ratio is 30. The specific mesh division of the flow field is shown in Fig. 1.

Fig. 2 shows the velocity contours of steady flow field at the velocities of the nozzle inlet $v$ = 5, 10,

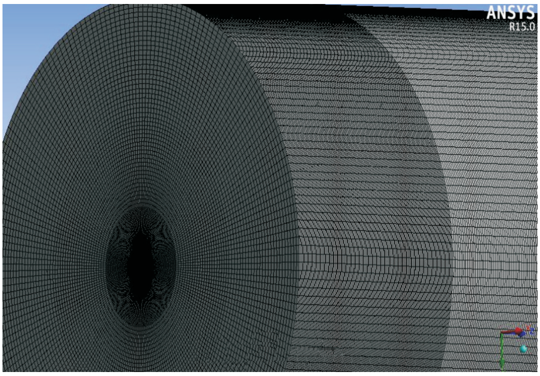


Fig.1 Fluid domain model

15 m/s. In Fig. 2, the structure of the time-averaged flow field is obvious, where the red area is the core area of the jet flow. The core length is about 80 mm,

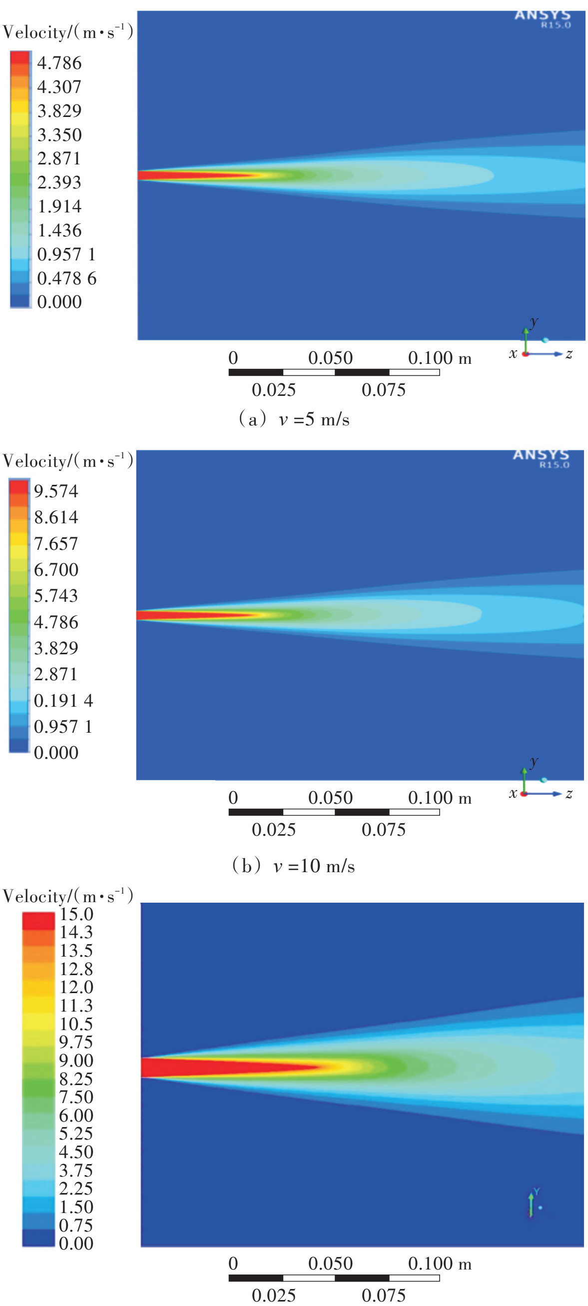


Fig.2 Steady flow velocity contours at different velocities

which is about 8 times the diameter of the nozzle. The result is consistent with that in Reference[9]. This indicates that in a certain range, the core length of the jet is independent of the nozzle velocity.

The data after the stabilization of the transient flow field can be used for the calculation of the sound field. It is supposed that the time step is $2\times10^{-4}$ s. We select the Ensight format, and save the data one time per time step.

## 2.2 Results and analysis of the sound field simulation

The computational domain is divided into three parts, i.e., the body source area, the sound propagation area, and the infinite element boundary, as shown in Fig. 3. The body source area is the flow field of the CFD calculation, and the media of both the sound propagation area and the body source area are water.

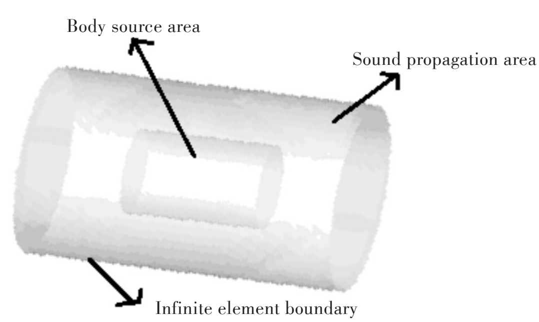


Fig.3 Schematic diagram of sound field calculation

To ensure the accuracy of sound wave, it is necessary to fill at least 6 meshes at one wavelength scale, which will substantially increase the amount of calculation in the sound field. Meanwhile, it will result in the mismatch between the calculation meshes of the flow field and the calculation meshes of the sound field. To carry out the sound field calculation, it is necessary to interpolate the calculation results of the flow field into the body source area.

The basic idea of the sound field calculation is shown in Fig. 4.

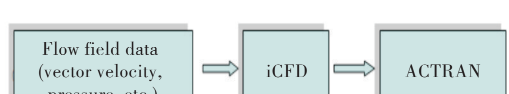


Fig.4 Flow chart of sound field calculation

According to the time step and saving interval of the transient flow field calculation, we can see that the maximum effective frequency of sound field calculation is 2.5 kHz, and the frequency resolution is 10 Hz. Based on the calculation results based on the

CFD flow field, we can obtain the sound pressure contours at different frequencies and with the inlet velocity of 15 m/s (see Fig. 5).

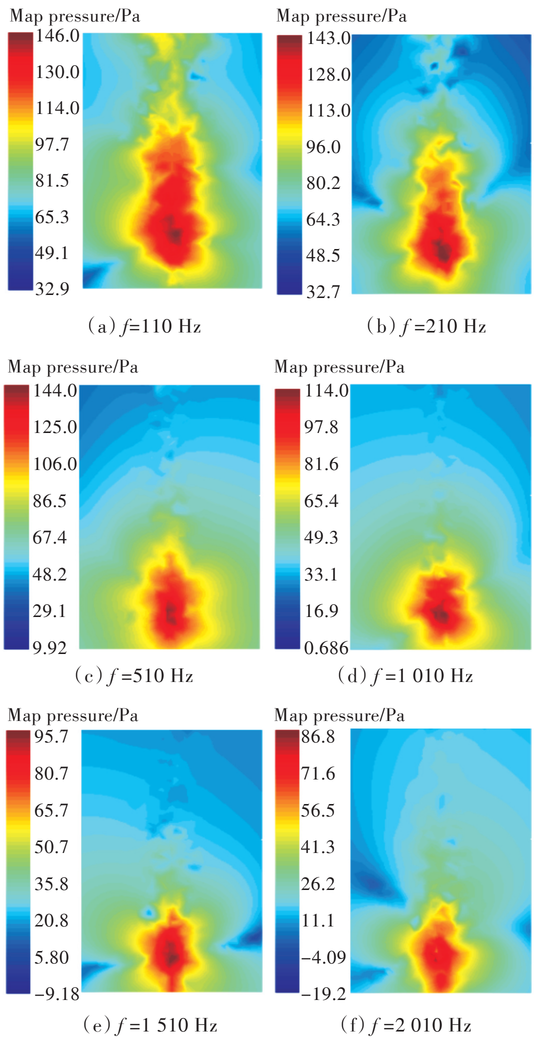


Fig.5 The sound pressure contours of inlet velocity of 15 m/s

From Fig. 5, we know that, the noise in the fluid domain mainly comes from the fully developed area. Moreover, as the frequency increases, the sound pressure level decreases and the directivity of the sound pressure field becomes worse. This is because the large-scale vortexes in the jet field are anisotropic, while the small-scale vortexes are isotropic. The large-scale vortexes are related to the generation of low-frequency noise and the small-scale vortexes are related to high-frequency noise.

Lighthill derived the famous $U^8$ law with the dimensional analysis, i.e., the radiant power of the turbulent jet noise is proportional to the jet velocity of eight powers when the jet velocity is low. Fig. 6 shows the radiated noise power spectra (0–2 kHz) when $v$ = 5, 10, 15 m/s. From the figure, we know that, as the frequency increases, the radiated noise power spectrum shows a decreasing tendency. As the flow velocity increases, the main contribution of the jet noise moves to the high frequency, i.e., the proportion of large-scale vortexes decreases and the proportion of small-scale vortexes increases. In Fig. 6, the Overall Sound Power Level (OSWL) is calculated according to the radiation power spectrum. From the result, we know that the OSWL is proportional to the flow velocity.

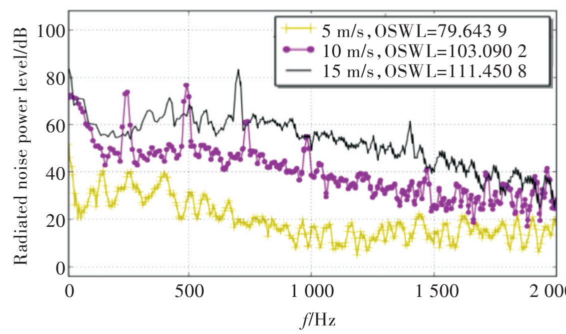


Fig.6 Radiated noise power spectrum at different velocities

Fig. 7 shows the relationship curve of the OSWL and the flow velocity. From Fig. 7, we know that, the numerical calculation result of the OSWL of the jet noise is basically consistent with the $U^8$ law, which theoretically verifies the accuracy of the calculation method for the radiation jet noise power.

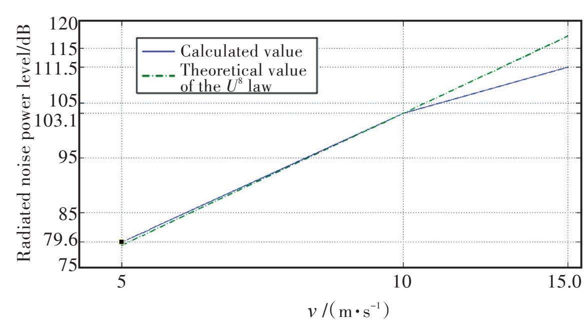


Fig.7 Comparison between numerical results and theoretical values of OSWL

## 3 Measurement experiment of underwater jet noise

The measurement experiment for the jet noise of nozzle is carried out in the reverberation tank with a size of 9 m × 3 m × 1.8 m. We adopt the reverberation method for the measurement[10]. The sound source level is

$$SL = \langle L_p \rangle - 10 \times \lg R \tag{9}$$

where $\langle L_p \rangle$ is the average sound pressure level in the reverberation control area; 10 × lgR is the correction for the results of the reverberation field measurement.

In the above equation,

$$R = S\left(e^{\frac{55.2V}{T_{60} S c_0}} - 1\right) \tag{10}$$

where $V$ is the internal volume of the reverberation tank; $S$ is the internal surface area of the reverberation tank; $c_0$ is the velocity of sound in water; the reverberation time of the reverberation tank is $T_{60}$ = 200 ms.

Therefore, to obtain the sound source level, we only need to measure the average sound pressure level of the reverberation field and make some correction on the results.

## 3.1 General situation of the experiment

The jet device used in the experiment is water supplied by the gravity type water tunnel tank, and the water is diverted to the reverberation tank by using the wired hose (see Fig. 8). Four standard hydrophones are set up in the static water area of the reverberation tank, and the space average technology is used to measure the jet noise signal of the nozzle with the diameter of 10 mm at different velocities.

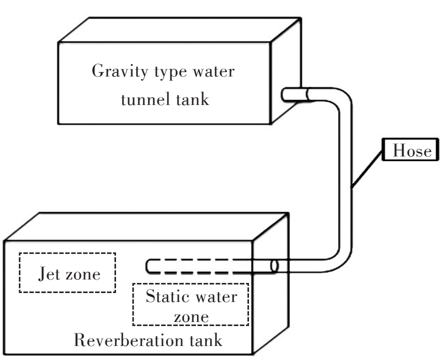


Fig.8 Schematic diagram of device connection

## 3.2 Experimental results

By adjusting the effluent velocity with the outlet valve, we separately measure the sound pressure signals of jet noise at different velocities. The experimental results are shown in Fig. 9.

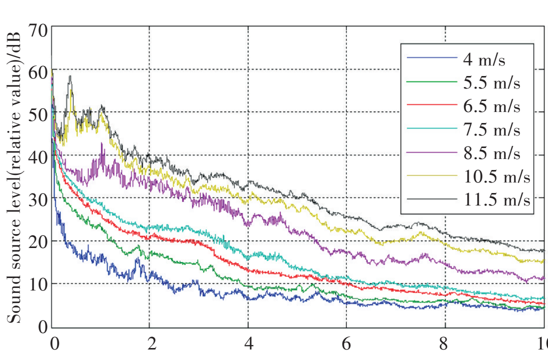


Fig.9 The results of flow noise source level at different velocities

By comparing the experimental results and the theoretical values of the radiation characteristics of the jet noise (see Fig. 10), we know that, the two are basically consistent. This indicates the effectiveness of the jet noise measurement with the reverberation method.

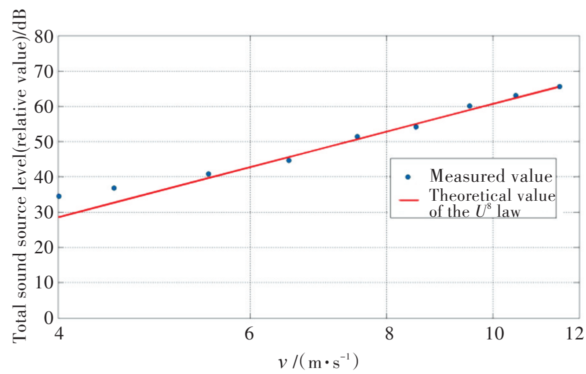


Fig.10 Comparison between experimental results and theoretical values of sound source level

# 4 Conclusions

Aiming at the underwater jet noise problem, we adopt the combined method of the LES and Lighthill acoustic analogy to carry out numerical simulation and experiment verification on the jet flow field and the sound field. Through research, we obtain the following conclusions:

1) The core length of the steady jet flow field is independent of the flow velocity, and the length is about 8 times the diameter of the nozzle.

2) The radiation power of jet noise is in accordance with the $U^8$ law, i.e., the radiation power is proportional to the flow velocity of eight powers.

3) The differences among the radiated noise power spectra at different flow velocities are great in the low frequency, while it is significantly reduced in the high frequency. The energy of the radiated noise is mainly concentrated in the low frequency. With the increase in the flow velocity, the main contribution of the jet noise moves to the high frequency, i.e., the proportion of large-scale vortexes decreases, while the proportion of small-scale vortexes increases.

# References

[1] MA D Y. Development of the law of turbulent jet noise [J]. Acta Acustica, 1987, 12(5): 321–328 (in Chinese).

[2] QIN W J, HU C G, GUO L P, et al. Effect of near-wall grid size on turbulent flow solutions [J]. Transactions of Beijing Institute of Technology, 2006, 26(5): 388–392 (in Chinese).

[3] BENSOW R E, PERSSON T, FUREBY C, et al. Large eddy simulation of the viscous flow around submarine hulls [C]//25th ONR Symposium on Naval Hy-

drodynamics. St. John's, Newfoundland and Labrador, Canada: Chalmers Publication Library, 2004.
[4] STANLEY S A, SARKAR S, MELLADO J P. A study of the flow-field evolution and mixing in a planar turbulent jet using direct numerical simulation[J]. Journal of Fluid Mechanics, 2002, 450(1): 377-407.
[5] PEI X, XU M, CHEN Z M. Exploring theoretically effect of coaxial nozzle flow on jet noise[J]. Journal of Northwestern Polytechnical University, 2011, 29(5): 772-776 (in Chinese).
[6] WANG C X, ZOU J, ZHANG T, et al. Experimental measurements of submerged free jet noise[J]. Journal of Ship Mechanics, 2010, 14(1/2): 172-180 (in Chinese).
[7] WANG X, ZHENG L, ZHOU Y R, et al. Flow field structure and noise for different nozzles[J]. Journal of Propulsion Technology, 2011, 32(3): 365-369 (in Chinese).
[8] TAM C K W, GOLEBIOWSKI M, SEINER J M. On the two components of turbulent mixing noise from supersonic jets[C]// Aeroacoustics Conference, Aeroacoustics Conferences. State College, PA, USA: AIAA, 1996: 96-1716.
[9] LIU P Q. Free Turbulent Jet Theory[M]. Beijing: Beihang University Press, 2008: 10-11(in Chinese).
[10] SHANG D J, LI Q, SHAGN D J, et al. Experimental investigation on flow-induced noise of the underwater hydrofoil structure[J]. Acta Acustica, 2012, 37(4): 416-423 (in Chinese).

# 轴对称直喷管的水下射流噪声特性数值模拟与实验验证

邢军华[1], 尚大晶[2], 张成[1], 苗天丞[1]
1 中国舰船研究设计中心 船舶振动噪声重点实验室，湖北 武汉 430064
2 哈尔滨工程大学 水声技术重点实验室，黑龙江 哈尔滨 150001

**摘　要：**[**目的**]为研究水下射流噪声特性，[**方法**]应用Lighthill声类比计算轴对称直喷管的自由射流声场特性，借助FLUENT仿真软件并采用大涡模拟法计算该直喷管的水下射流流场，最后基于混响法进行实验验证。[**结果**]结果表明：稳态射流流场的核心区长度与流速无关，核心区长度约为喷管直径的8倍；射流噪声辐射功率与流速的8次幂成正比；不同流速下的射流噪声功率谱在低频段的差异较大，在高频段的差异则显著减小，且辐射噪声能量主要集中在低频段，但流速增加后射流噪声的主要贡献将向高频段移动。[**结论**]在射流噪声计算仿真方面，将大涡模拟法和Lighthill声类比相结合是一种有效的分析手段。

**关键词：**轴对称直喷管；射流噪声；混响法